

Organic metal halide perovskite has recently shown great potential for applications, as it has the advantages of low cost, excellent photoelectric properties, and high power conversion efficiency. The Hole Transport Material (HTM) is one of the most critical components in Perovskite Solar Cells (PSC). It has the function of optimizing the interface, adjusting the energy compatibility, and obtaining higher PCE. The inorganic p-type semiconductor is an alternative HTM due to its chemical stability, higher mobility, increased transparency in the visible region, and general valence band energy level (VB). Here we report the use of the Graphene Oxide (GO) layer as a Hole Transport Layer (HTL) to improve the perovskite solar cells' performance. The crystal structure and thickness of GO significantly affect the increase in solar cell efficiency. This perovskite film must show a high degree of crystallinity. The configuration of the perovskite material is FTO/NiO/GO/CH₃NH₃PbI₃/ZnO/Ag. GO as a Hole Transport Layer can increase positively charged electrons' mobility to improve current and voltage. As a blocking layer that can prevent recombination. The GO can make the perovskite interface layer with smoother holes, and molecular uniformity occurs to reduce recombination. The method used in this study is by using spin coating. In the spin-coating process, the GO layer is coated on top of NiO with variations in the rotation of 700 rpm, 800 rpm, 900 rpm, 1,000 rpm, and 1,500 rpm. The procedure formed different thicknesses from 332.5 nm, 314.7 nm, 256.4 nm, 227.4 nm to 204.5 nm. The results obtained at a thickness of 227.4 nm reached the optimum efficiency, namely 15,3%. Thus, the GO material as a Hole Transport Layer can support solar cell performance improvement by not being too thick and thin

Keywords: perovskite solar cells, hole transport layer, graphene oxide, thickness, performance

UDC 616

DOI: 10.15587/1729-4061.2021.225420

PERFORMANCE OF PEROVSKITE SOLAR CELL COATED WITH GRAPHENE OXIDE AS HOLE TRANSPORT LAYER

Rustan Hatib

Doctoral Student in Mechanical Engineering*

E-mail: rustanhatib98@gmail.com

Sudjito Soeparman

Professor in Mechanical Engineering*

E-mail: sudjitosp@ub.ac.id

Denny Widhiyanuriyawan

Doctorate in Mechanical Engineering*

E-mail: Denny_w@ub.ac.id

Nurkholis Hamidi

Doctorate in Mechanical Engineering*

E-mail: hamidy@ub.ac.id

*Department of Mechanical Engineering

Brawijaya University

Jl. Majjend Haryono, 167, Malang, Indonesia, 65145

Received date 28.12.2020

Accepted date 03.02.2021

Published date 26.02.2021

Copyright © 2021, Rustan Hatib, Sudjito Soeparman, Denny Widhiyanuriyawan, Nurkholis Hamidi

This is an open access article under the CC BY license

<http://creativecommons.org/licenses/by/4.0>

1. Introduction

Solar energy is an alternative energy source to meet global energy needs in today's life. In this regard, photovoltaic technology is the best choice to face the global energy crisis because of its eternal nature. Solar cells, or also called photovoltaic cells (PV), are a technology that can convert solar energy in the form of photons into electrical energy. The process of converting electrical energy in PV utilizes photons in sunlight at visible light wavelengths to excite electrons in semiconductor materials so that electrons' flow occurs.

Several generations of solar cells have been produced, each of which has advantages and disadvantages. There are several things that concern PV technology, including stability, ease in the fabrication process, and especially energy efficiency. Currently, perovskite-type solar cells (PSC) made from organic (CH₃NH₃) and inorganic (PbX₃, X=Br, Cl, I) matters have attracted the attention of researchers because they can dramatically increase efficiency from 3.9% in 2009 to 22.1% at present [1]. PSC also can absorb photons with a power conversion of more than 30% [2], its simple structure and potential application to flexible substrates [3]. The advantages of PSC-type PV cells were described in full by [4], who stated that PSCs had good film formation prop-

erties, good transparency, and were close to infrared. Hole Transport Material (HTM) is an advantage of PSC as an electric charge layer, which significantly affects its efficiency increase due to its good transparency [5]. Next, we will describe some of the research results related to HTL and PSC.

From several research results, inorganic materials that are widely used as HTL are CuSCN [6], NiO [7], CuO [8], and MoO₃ [9]. The wide usage is due to the excess of inorganic materials compared to organic in terms of the higher mobility of the holes and a broader bandgap that could absorb more photons. Meanwhile, the advantages of modern organic materials, such as Poly(3,4-ethylene dioxythiophene): polystyrene sulfonate (PEDOT: PSS) as HTL PSC, are only in terms of efficiency of PSC cells. Unfortunately, this good efficiency does not last long due to its acidity, its tendency to absorb water, and especially its inability to block electrons [10]. Therefore, inorganic materials are still a better choice as HTL PSC compared to organic materials.

The HTL material criteria include that the valence bond in HTL must synchronize with the perovskite's valence bond to reach high Voc. The mobility of the hole must be acceptable to increase the fill factor, and good thermal stability. Another criterion that must be considered is the thickness of the HTL, which can improve PSC growth. Based on the

above criteria, [11] developed several organic and inorganic hole transport materials on the PSC.

From the description above, interesting things that need to be investigated are related to the type of HTL material that supports increased stability and efficiency of PSC by looking at electron mobility, blocking layer properties, and the ability to induce ions in perovskite material that generate electrons rapidly. One way to increase PSCs' efficiency and stability is to add graphene oxide (GO) as HTL. It can be seen in the PSC working principle, where when the perovskite layer absorbs photons, positive ions will be excited faster with the addition of GO. In contrast, negative ions will go to the electron transport layer (ETL). As a result, there will be a uniformity of the atoms in the perovskite, increasing the electric current. The problem with the addition of GO as HTL is the synchronization of the value of the layer thickness and the PSC optimal rotation speed.

2. Literature review and problem statement

Research related to inorganic material types of GO and perovskite as a combination of inorganic and organic has been carried out by [12]. They combined these two materials at various GO concentrations, while perovskite material at a constant concentration. The efficiency obtained was 15.2. % at a concentration of 50 % GO. In this study, the GO solution's concentration was constant, but the GO layer's thickness was varied from the size of different spin coatings. It is essential to get the thickness synchronization of GO in nm units and spin coating in rpm to get the best efficiency. GO here functions as HTL, which is positioned below the perovskite material.

Researchers have conducted several studies using inorganic materials other than GO as HTL. The research that used sol-gel NiO nanocrystal (NC) material as the hole transport layer that was conducted by [13] can form well-crystallized perovskite layers. NiO nanocrystal inorganic material produced the best PSC efficiency, namely 9.11 % at a thickness of 30 and 40 nm using the doctor blade method. Meanwhile, the thicknesses of 20 nm and 70 nm have lower efficiency, namely 6.04 % and 5.58 %, respectively. At a low thickness of 20 nm, there is a chance of large leakage currents so that the low fill factor causes low efficiency, while at a high thickness of 70 nm, higher resistance can occur. This research is quite informative, but needs to be tested for different methods and materials, whether it is still consistently showing high efficiency at 30 and 40 nm thickness. Meanwhile, a study using Spiro-OMeTAD material conducted by [14] stated that 180 nm HTL thickness resulted in optimal efficiency of around 15.5 % and decreased efficiency to 10.8 % if the thickness was above 180 nm. Unfortunately, this study does not display the number of the round in the HTL thickness, but only says that the rotation is varied. It appears that the thickness of the HTL layer is an essential part of an anticipatory step to avoid recombination. However, whether HTL thickness is a major determinant of increasing PSC efficiency, further investigation is needed to conclude this.

Furthermore, [15] describes the results of her research using the spiro-OMeTAD material at various rotational speeds; 100 nm, 4000 rpm; 200 nm, 2,000 rpm; and 400 nm, 700 rpm with a layer of HTL solution on the perovskite surface for 20 seconds. The rotation speed ratio and the thickness of the material show that the increase in rotation is accompanied by a decrease in thickness (2,000 rpm, 200 nm; 4,000 rpm, 100 nm). But what becomes a question

mark at 700 rpm, why is it much thicker to 400 nm. Hypothetically, this will slow down coating time. Next for 50 nm, the spiro-OMeTAD concentration was reduced by half, while the additive ratio remained the same, and the solution was coated at 4000 rpm for 20 seconds. Analogously, the spiro-OMeTAD concentration file increased by 1.5 to 600 nm, the additive ratio remained the same, and the solution was coated with a spin at 700 rpm for 20 seconds. The results obtained are that the optimum efficiency is 13.5 % at 2,000 rpm rotation with a thickness of 200 nm.

Therefore, this research will investigate Graphene Oxide's performance (GO) as the Hole Transport Layer (HTL) in the Spin-Coating Process on the PSC. The rotation and thickness of the HTL are synchronized to get the best performance, which results in optimum efficiency with good current-voltage stability.

3. The aim and objectives of the study

This study aims to determine the optimal thickness of Graphene Oxide which functions as a Hole Transport Layer which can increase the efficiency of the PSC.

To achieve this goal, the following objectives are formulated:

- measuring the current and voltage of the PSC in spin coated variations of GO 700, 800 900, 1,000 and 1,500 rpm;
- testing the properties of the GO hole transport layer by SEM;
- tested GO crystal grain display with XRD.

4. Materials and methods

NiO film was made by mixing Nickel Acetate Tetrahydrate and Monoethanolamine into ethanol, both at a concentration of 0.1M. The mix was then stirred on a hot plate at 70 °C for 4 hours until the conditions are homogeneous and green. The same has been done by [16]. Then, 2 mg/ml of graphene oxide (Sigma Aldrich). Then to get a concentration of 2 mg/ml GO obtained from Sigma Aldrich. In fact, GO is an inorganic material that is an insulator, so to eliminate this property it is necessary to reduce it by using chemicals and heat treatment methods that can generate electric energy [17–20]. In other words, GO which is an insulator must be reduced with certain treatments to convert it into rGO, which is a conductor that produces electrical power.

Meanwhile, Methylammonium Iodide (MAI) solution is made by dissolving 90 mg of MAI powder in 2 ml of isopropanol (IPA) solvent known as isopropyl alcohol (2-propanol). Lead Iodide (PbI₂) solution was prepared by dissolving 900 mg of PbI₂ powder in 2 ml of N-N-Dimethylformamide (DMF) solvent, then stirred at 70 °C for 24 hours. Centrifugation is necessary before use to obtain a clear PbI₂ solution.

ZnO nanoparticles were made; namely, zinc acetate dehydrates (2.95 g, 13.4 mmol) into methanol (125 ml) then stirred at 65 °C. KOH (1.48 g, 23 mmol) into methanol (65 ml) heated at 60–65 °C for 15 minutes. Then the reaction was mixed and stirred for 2.5 hours at 65 °C. After that, it was cooled to room temperature. Before use, ZnO nanoparticles were filtered first using a 0.45 µm PVDF syringe filter [21].

The technique used in this research is a variation of the GO rotation as HTL on the PSC structure. The variations of the GO rotation are 700 rpm, 800 rpm, 900 rpm, 1,000 rpm and 1500 rpm.

The final process includes the fabrication of Solar Cells on FTO glass substrates. The FTO pattern was cleaned ultrasonically with acetone, detergent, and acetone again, followed by UV-Ozone Cleaner for 25 minutes [22]. NiO film deposition was carried out by spin-coating at 1,000 rpm for 60 seconds on the FTO glass substrate. After that, it was annealed at 250 °C for 30 seconds. The GO solution was spin-coated at 700 rpm, 800 rpm, 900 rpm, 1,000 rpm, and 1,500 rpm for 60 seconds, after which it was annealed at 200 °C for 60 minutes. The perovskite spin-coating process began with spin-coating of the PbI₂ solution at 1,000 rpm for 30 seconds. Then, the MAI solution was spin-coated on top of the PbI₂ layer at a speed of 1,000 rpm for 30 seconds. As a result, there was a conversion from PbI₂ to CH₃NH₃PbI₃ perovskite that was then annealed at 100 °C for 20 seconds. ZnO nanoparticle coating was spin-coated on the substrates at 1,000 rpm for 30 seconds. The results of the film are dark brown and following what was done by [23]. Finally, about the thickness of 100 nm, the electrode's silver layer was attached using a thermal evaporator at a pressure of 1×10⁻⁶ mbar. The two sides were set in the binder clip to keep the cell structure in good condition. For this reason, PSC solar cells are ready to be tested.

Tests were carried out in the form of measuring currents and voltages using a data logger to determine the performance of solar cells. Scanning Electron Microscope (SEM, FEI Inspect-S50) was used to investigate cross-sectional morphology of the solid-state devices. X-ray diffraction (XRD) pattern was obtained using a PANalytical/X'Pert PRO diffractometer with Cu K α radiation at a scan rate of 0.02°/s in the 2 θ range from 10° to 90° under operation conditions of 40 kV and 35 mA. In terms of sample analysis in this study, the XRD used was compared with the Raman Spectroscopy method. XRD can analyze samples quickly because it does not need to heat through laser radiation, which can damage the sample. This means that XRD has a high sensitivity. Besides, XRD can be used to analyze metals or alloys and can reveal the microstructure lattice and crystal phase of the sample [24]. However, XRD also has limitations in terms of the size crystal structure. The usual small structures are not readable by XRD [25].

GO thickness is obtained from variations in rotation. Each rotation produces a different thickness of the GO. GO thickness measurements can be made by cutting the fabricated sample to obtain a clear surface. The sample to be analyzed is placed in a holder measuring ±10 mm. Then the sample is placed into the SEM chamber. The test equipment will display the results of the material layer thickness readings on the computer screen. This is known by using the SEM cross-section tool. This can be seen in Fig. 4.

Fig. 1, *a* shows the fabricated structure of perovskite solar cells. The perovskite solar cell structure contains several parts, namely Fluorine Tin Oxide conductor glass as an electrode work substrate, NiO as Hole Transport Layer 1 for stabil-

ity, Graphene Oxide is a level 2 Hole Transport Layer, which functions to accelerate the flow of positively charged electrons and can block negatively charged electrons, perovskite layer to absorb photons, ZnO as Electron Transport layer and Ag as a counter electrode. The PSC mechanism with the addition of Graphene Oxide as HTL can be seen in Fig. 1, *b*.

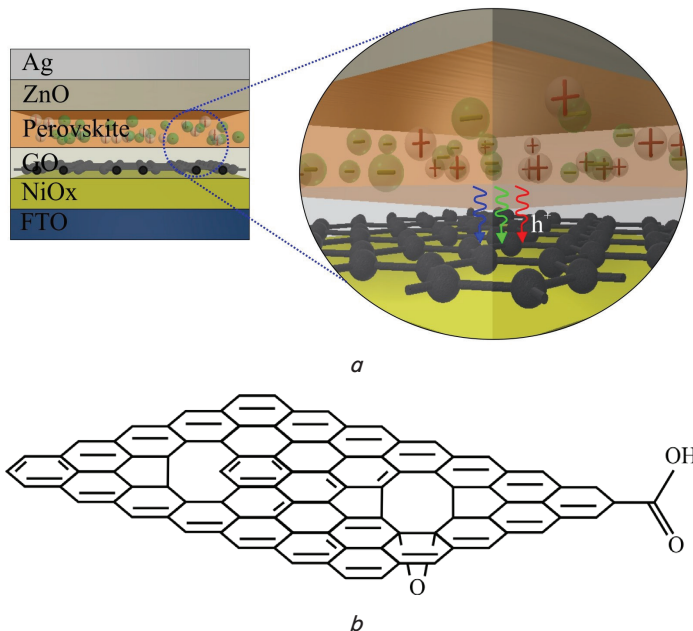


Fig. 1. PSC device configuration: *a* – fabricated structure of PSC; *b* – mechanism of electron transfer from perovskite to GO; *c* – GO structure

When the perovskite layer absorbs light, there will be ions: positive ions and negative ions. Electrons that are positively charged will go to HTL, and those negatively charged will go to ETL. Graphene Oxide as HTL serves to increase the mobility of positively charged electrons. The increase in electron mobility causes an increase in current and voltage. Besides, GO also functions as a blocking layer to prevent electron recombination.

A test scheme was carried out to determine the amount of electrical energy produced by the PSC, as shown in Fig. 2.

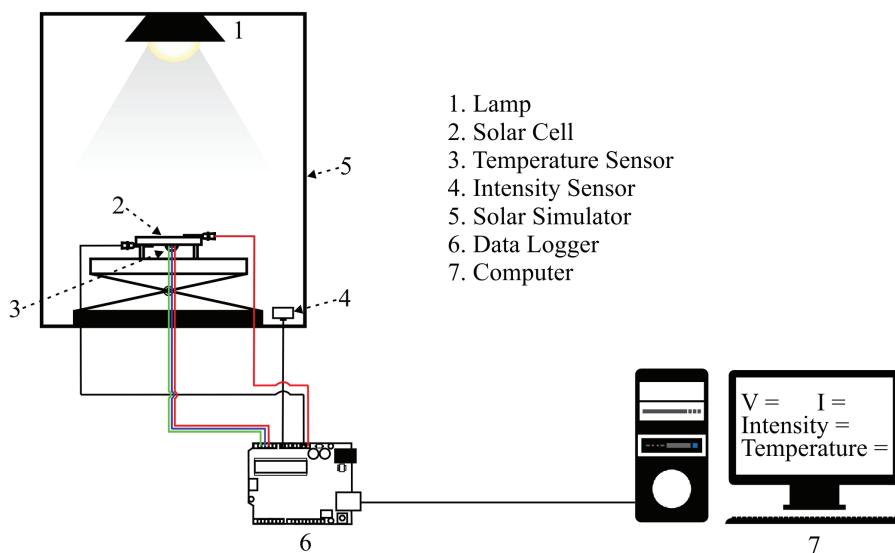


Fig. 2. Research equipment installation

As seen in the research installation image above, the PSC current and voltage is a radiation generator consisting of a halogen bulb in a solar simulator (1). Perovskite solar cells are objects in this study used to determine performance (2). Temperature sensors were used to measure the temperature of solar cells (3). Intensity sensors were used to measure the intensity of halogen lamp radiation (4). A solar simulator was used as a solar cell measurement (5). The current and voltage were measured using a data logger to determine the PSC's performance (6). The computer is a tool to test the current and voltage generated by the PSC.

5. Results of the research on increasing the efficiency of perovskite solar cells with graphene oxide as the hole transport layer

To get the efficiency results of perovskite solar cells with graphene oxide as the hole transport layer, several tests were carried out.

5.1. Current and voltage testing with variations in the thickness of Graphene Oxide

The fabrication device's photovoltaic characteristics were characterized under simulation A.M. 1.5 illuminations at 100 mW/cm^2 . The plot of device current voltages is shown in Fig. 3. The average short-circuit current density (J_{sc}), open-circuit voltage (V_{oc}), fill factor (ff), and power conversion efficiency values for each set of devices are summarized in Table 1.

Table 1

Comparison of GO thickness in HTL

Spin Coated (rpm)	Thickness GO (nm)	Voc (V)	Isc (mA/cm^2)	FF	PCE (%)
700	332.5	0.72	16.8	64.12	7.76
800	314.7	0.797	16	66.97	8.54
900	256.4	0.745	17.7	73.58	9.7
1000	227.4	0.982	17.9	87.04	15.3
1,500	204.5	0.923	16.7	77.2	11.9

The data in Table 1 shows variations in the thickness of the thin film GO and spin-coated rotation, which affect the efficiency of the PSC's electrical energy conversion. The lowest efficiency was obtained at the lowest rotation (7.76 %: 700 rpm). The highest efficiency was not obtained at the highest rotation but 1,000 rpm with an efficiency of 15.3 %. It can be concluded that synchronization occurs between rotation and thickness of GO at 1,000 rpm, not 1,500 rpm.

5.2. Testing SEM cross-section with GO as HTL

A uniform thin film was coated on the FTO glass using spin coating to determine the transport properties of the GO in PSC holes. Fig. 3, *a–e* show SEM images of the resulting hole transport layer with spin-coatings at 700 rpm, 800 rpm, 900 rpm, 1,000 rpm, and 1,500 rpm, respectively. Fig. 3 shows the corresponding top view in each image.

The SEM image shows that the PSC is uniform, smooth, with a well-crystallized and packed granule. The procedure formed different thicknesses from 332.5 nm, 314.7 nm, 256.4 nm, 227.4 to 204.5 nm. Fig. 4 shows an SEM cross-section photo showing the material's layer arrangement where the GO's thickness is visible.

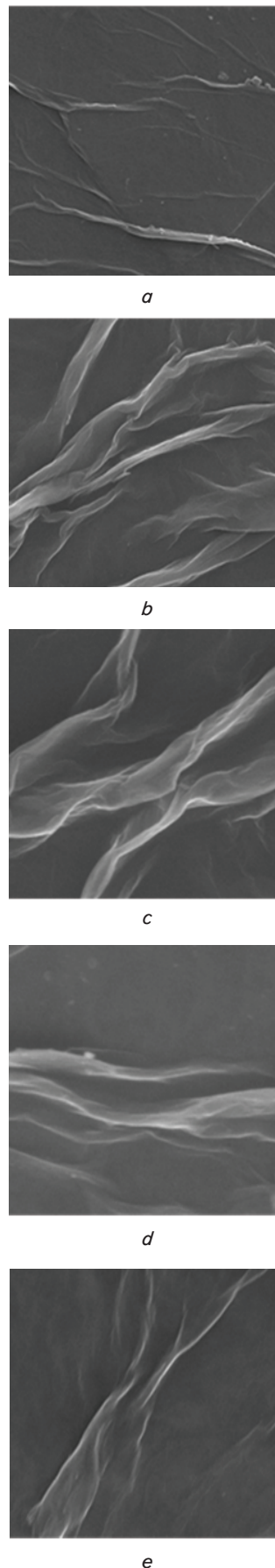


Fig. 3. SEM image of PSC at GO variation: *a* – 332.5 nm; *b* – 314.7 nm; *c* – 256.4 nm; *d* – 227.4; *e* – 204.5 nm

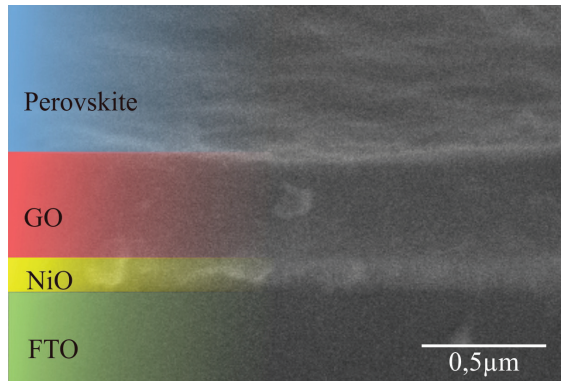


Fig. 4. SEM cross-section PSC

Fig. 4 shows a cross-sectional SEM image of glass film/FTO/NiO/GO/CH₃NH₃PbI₃. To prepare this film, we apply a deposition method with a spin coating. Variations in thickness can easily distinguish the GO layer.

5. 3. XRD testing with GO as HTL

The XRD patterns of the GO samples made at various cycles are shown in Fig. 5.

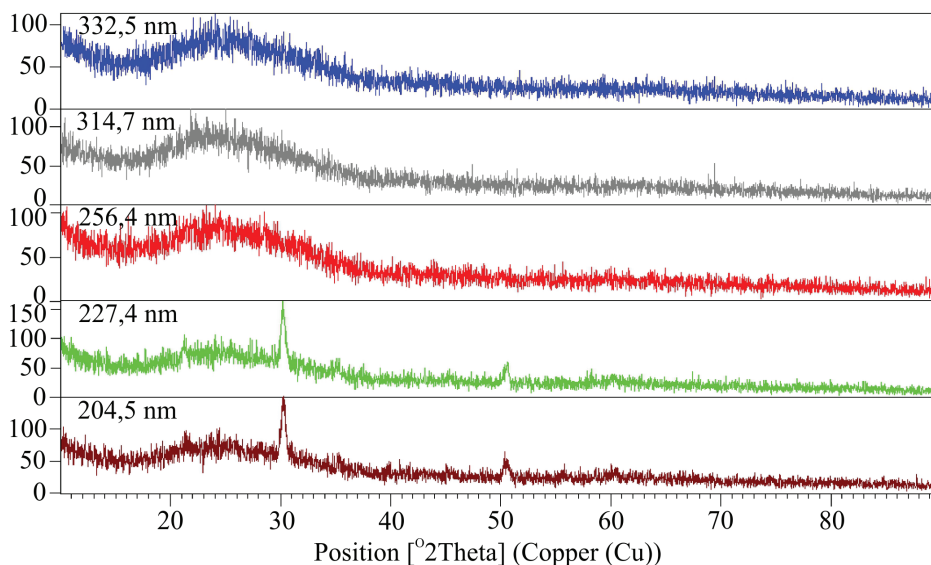


Fig. 5. XRD on the PSC with variations in GO thickness

At rotation between 700 and 900 rpm, the diffraction peaks are still weak, and the crystals are not visible. This means that the amount of rotation is still amorphous. Furthermore, at rotations above 900 rpm (1,000 and 1,500 rpm), crystal grain growth has started to occur, indicated by a small peak at 2θ around 50° . Later at 2θ about 30° , the appearance of the crystalline granules will be better. The same thing was obtained by [14] at a heating treatment of 900°C .

6. Discussion of the thickness variation of GO as HTL in perovskite solar cells

6. 1. Discussion of the results of thickness variations of GO by testing current and voltage against optimal efficiency in perovskite solar cells

Fig. 6 shows the effect of GO thickness as HTL on PSC devices performance. The thickness of the GO layer

is obtained from the spin-coating variation method. It can be seen that on the device, the thickness of the GO is 227.4 nm, the Voc, Isc, and FF values are optimal so that the highest PCE is also obtained. Devices that use a 332.5 nm thick GO layer have slightly lower device performance; hence, the PCE is also small, as can be seen in Fig. 7. At 227.4 nm thickness, the average voltage is 0.97 V, current 17.9 mA/cm², fill factor 78 %, and PCE 14 %. The thick GO film absorbs a lot of light but contributes little to the Isc currents. Due to the large series resistance to the device, it causes the fill factor to drop. Also, if the thickness of GO is 204.5 nm, the efficiency will be low (11.9 %). It is due to the low absorption of light, where the electrons move slowly. The GO thin layer can cause the perovskite material to quickly penetrate the NiO layer under the GO so that electron recombination can occur.

It can be briefly described that the GO thin film at 227.4 nm thickness deposited on top of the NiO layer is an effective hole transport layer in the PSC. The PSC device's efficiency value obtained by varying the thickness of GO as HTL is comparable to that of devices made on NiO to support the growth of perovskite material. If we look at the test conducted by [14] on the Spiro OMeTAD material, the highest efficiency at 180 nm thickness is 15.5 %.

However, the efficiency will decrease if the thickness is above 180 nm. Likewise, in [15], the highest efficiency obtained was at a thickness of 200 nm with a rotation of 2000 rpm. It means that GO as HTL still produces the highest efficiency at 227.4 nm thickness. It is because GO is based on the carbon element with a unique property, namely the ability to induce electrons with a greater positive charge. The thermal treated GO has properties similar to the reduction of GO. GO reduction has a tiny band gap, so it is capable of swift electron transfers. It is what causes an increase in electric

current and voltage. Uniquely, PSC efficiency decreases when the GO's thickness is below 227.4 nm (204.7 nm) and above 227.4 nm (332.5 nm). These results indicate the importance of paying attention to GO concentration. During testing, the GO solution's concentration when in spin-coating was still not optimal for the cross-sectional area of conductive glass. It is a recommendation for further research on the amount of solution concentration with the cross-sectional area. It should be noted that the amount of concentration of GO solution dramatically affects its ability to induce positive ions in perovskite material, as well as its ability to block negatively charged electrons.

Recent developments in the deposition of highly uniform thin films with thickness values ranging from a single layer as HTL to two layers or bilayers in large area HTL make it easy to include GO as HTL on PSCs. In this study, GO as a bilayer layer aims to increase electron mobility, which can increase the current and voltage as shown in Table 1.

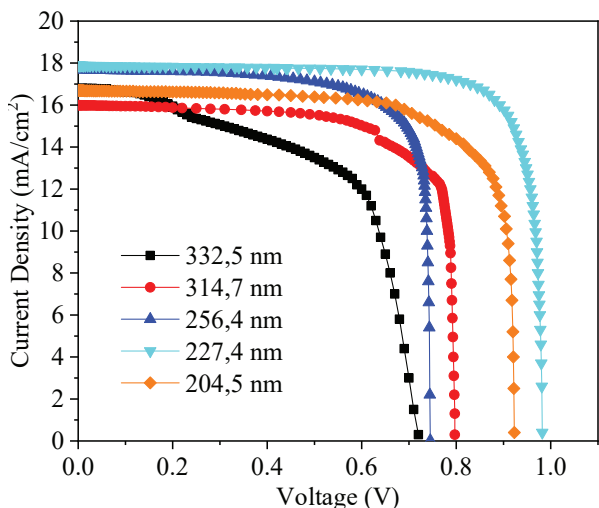


Fig. 6. Representative $J - V$ curves of PSC with thickness variation

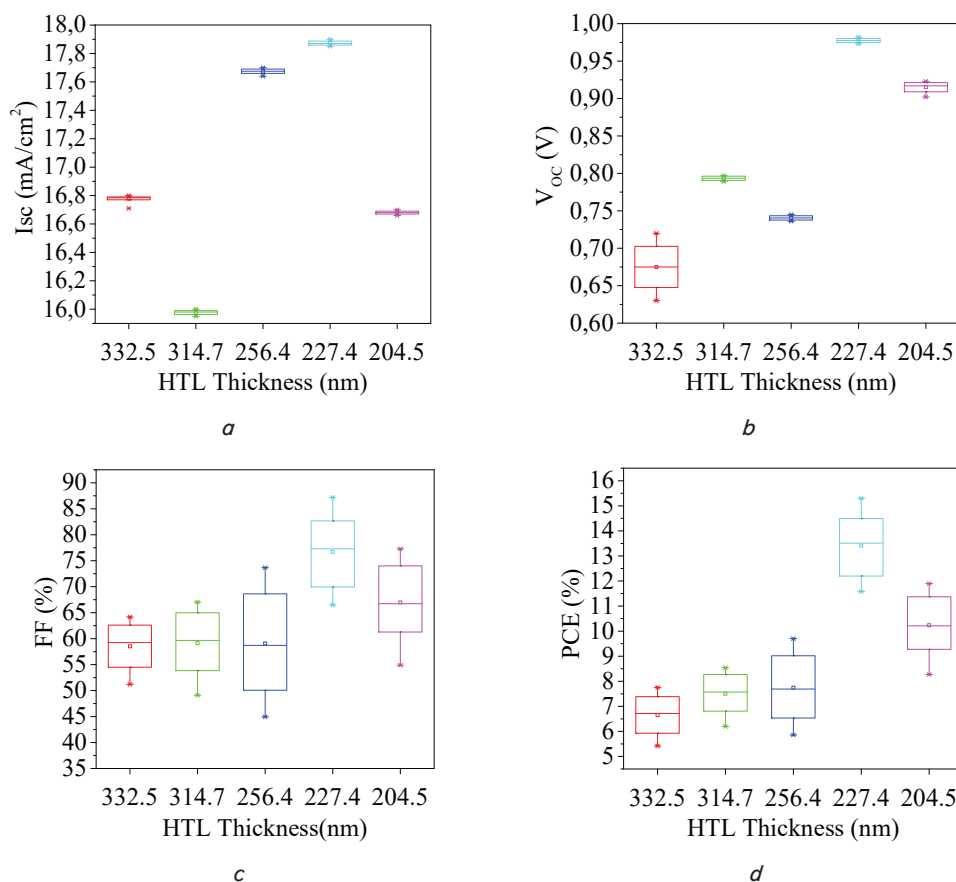


Fig. 7. PSC performance statistics using thickness variations of GO as HTL: $a - V_{oc}$, $b - J_{sc}$, $c - FF$, $d - PCE$

The limitation in this research is the rotation variation of 700, 800, 900, 1,000 and 1,500 rpm. The concentration of the solution is 100 μl . GO heating time is 60 minutes at a temperature of 200 $^{\circ}\text{C}$.

From the results of this study, there are several things that need to be developed, namely variations in rotation that should be neatly arranged, for example, 700, 800, 900, 1,000, 1,100, 1,200, 1,300, 1,400 and 1,500 rpm. The total concentration of the solution must correspond to the area of

the FTO conductive glass substrate. The GO heating time needs to be varied to get a result that is close to rGO. This is done to get optimal efficiency.

6. 2. Discussion of the results of thickness variation of GO with SEM testing

The 3D figure above shows a well-crystallized cubic phase of the $\text{CH}_3\text{NH}_3\text{PbI}_3$ perovskite layer formed on top of the GO layer. The clear cubic phase occurs at low thickness. This figure shows that a thicker layer of denser and larger cubic $\text{CH}_3\text{NH}_3\text{PbI}_3$ crystals can be formed in the GO layer. The film's surface roughness plays a large role in directing the perovskite layer's growth, especially for depositions using spin coating. Understandably, the roughness causes PbI_2 to be deposited in a relatively thick layer and is well connected by a high-speed spin layer. Thanks to this dense, well crystallized, interconnected, and thick layer of $\text{CH}_3\text{NH}_3\text{PbI}_3$, perovskite solar cells based on the GO layer can provide higher efficiency due to higher currents and voltages.

The limitation in this study is the measurement of the GO surface against the growth of the perovskite layer using SEM testing. However, to get the composition of elements in a sample surface, EDS (Energy-Dispersive X-ray Spectroscopy) is used. The aim is to determine the composition of the elements in the PSC, especially the carbon content.

6. 3. Discussion of microstructure characteristics of GO synthetic materials

Referring to Fig. 5, it appears that the XRD pattern on the spin coating from 700 to 900 rpm has no evident difference. It indicates that the GO aromatic layer's build-up structure is increased, or the structure that has not been evenly distributed is still amorphous. While at 1000 rpm and 1500 rpm, the XRD pattern has appeared at an angle of $2\theta=30^{\circ}$ and 50° . So, in this case, crystallization has occurred. The appearance of these peaks causes the atomic crystals to begin to arrange neatly. The narrower and higher the peak, the better the size and slice of the aromatic layer [14]. If the atomic crystal crystals are neatly arranged, photons' absorption is optimal, causing a high fill factor. The high fill factor will affect the increase in solar cell performance. Based on the theory and XRD results above, it can be seen that some microcrystalline GO structures are microscopic at low rotation. The XRD re-

sults suggest the successful conversion of GO precursors into rGO and graphene layers.

The limitation in this study is the measurement of GO crystals using XRD. However, to obtain smaller nano-sized GO crystals measurements used Raman Spectroscopy.

7. Conclusions

1. The spin-coated GO variations on the PSC resulted in an increase in current and voltage at the PSC with the highest current and voltage values, namely 17.9 mA/cm² and 0.982 V at 1,000 rpm. The increase in current and voltage causes the efficiency to increase by 15.3 %. The increase in current is due to the faster ability of GO as electron mobility.

2. The variation of spin-coated GO on PSC causes morphological changes in the hole transport layer, namely

the increasing rotation causes the roughness of the GO surface to be uniform, smooth and crystallized so that the relationship between the GO layer and perovskite layer is good.

3. The variation of spin-coated GO on the PSC causes the formation of GO crystal structures due to the high rotation of 1,000 rpm and 1,500 rpm. At 1,000 rpm and 1,500 rotation, crystals have been formed at an angle of $2\theta=30^\circ$ and 50° . This is due to the subtle variability of the GO surface.

Acknowledgments

The author expresses his gratitude to the Endowment Fund for Education (LPDP) of the Ministry of Finance of the Republic of Indonesia in which its Excellence Scholarship for Indonesian Lecturers – Domestic Program (BU-DI-DN) No. 20161141011768 has supported this research.

Reference

- Kojima, A., Teshima, K., Shirai, Y., Miyasaka, T. (2009). Organometal Halide Perovskites as Visible-Light Sensitizers for Photovoltaic Cells. *Journal of the American Chemical Society*, 131 (17), 6050–6051. doi: <https://doi.org/10.1021/ja809598r>
- Yang, W. S., Noh, J. H., Jeon, N. J., Kim, Y. C., Ryu, S., Seo, J., Seok, S. I. (2015). High-performance photovoltaic perovskite layers fabricated through intramolecular exchange. *Science*, 348 (6240), 1234–1237. doi: <https://doi.org/10.1126/science.aaa9272>
- Chiang, Y.-F., Jeng, J.-Y., Lee, M.-H., Peng, S.-R., Chen, P., Guo, T.-F. et. al. (2014). High voltage and efficient bilayer heterojunction solar cells based on an organic–inorganic hybrid perovskite absorber with a low-cost flexible substrate. *Phys. Chem. Chem. Phys.*, 16 (13), 6033–6040. doi: <https://doi.org/10.1039/c4cp00298a>
- Yip, H.-L., Jen, A. K.-Y. (2012). Recent advances in solution-processed interfacial materials for efficient and stable polymer solar cells. *Energy & Environmental Science*, 5 (3), 5994. doi: <https://doi.org/10.1039/c2ee02806a>
- Vivo, P., Salunke, J., Priimagi, A. (2017). Hole-Transporting Materials for Printable Perovskite Solar Cells. *Materials*, 10 (9), 1087. doi: <https://doi.org/10.3390/ma10091087>
- Niu, G., Li, W., Li, J., Wang, L. (2016). Progress of interface engineering in perovskite solar cells. *Science China Materials*, 59 (9), 728–742. doi: <https://doi.org/10.1007/s40843-016-5094-6>
- Shang, Y., Hao, S., Yang, C., Chen, G. (2015). Enhancing Solar Cell Efficiency Using Photon Upconversion Materials. *Nanomaterials*, 5 (4), 1782–1809. doi: <https://doi.org/10.3390/nano5041782>
- Kim, J. H., Liang, P.-W., Williams, S. T., Cho, N., Chueh, C.-C., Glaz, M. S. et. al. (2014). High-Performance and Environmentally Stable Planar Heterojunction Perovskite Solar Cells Based on a Solution-Processed Copper-Doped Nickel Oxide Hole-Transporting Layer. *Advanced Materials*, 27 (4), 695–701. doi: <https://doi.org/10.1002/adma.201404189>
- Frost, J. M., Butler, K. T., Brivio, F., Hendon, C. H., van Schilfgaarde, M., Walsh, A. (2014). Atomistic Origins of High-Performance in Hybrid Halide Perovskite Solar Cells. *Nano Letters*, 14 (5), 2584–2590. doi: <https://doi.org/10.1021/nl500390f>
- Zhang, P.-P., Zhou, Z.-J., Kou, D.-X., Wu, S.-X. (2017). Perovskite Thin Film Solar Cells Based on Inorganic Hole Conducting Materials. *International Journal of Photoenergy*, 2017, 1–10. doi: <https://doi.org/10.1155/2017/6109092>
- Rajeswari, R., Mrinalini, M., Prasanthkumar, S., Giribabu, L. (2017). Emerging of Inorganic Hole Transporting Materials For Perovskite Solar Cells. *The Chemical Record*, 17 (7), 681–699. doi: <https://doi.org/10.1002/ter.201600117>
- Chung, C.-C., Narra, S., Jokar, E., Wu, H.-P., Wei-Guang Diao, E. (2017). Inverted planar solar cells based on perovskite/graphene oxide hybrid composites. *Journal of Materials Chemistry A*, 5 (27), 13957–13965. doi: <https://doi.org/10.1039/c7ta04575a>
- Zhu, Z., Bai, Y., Zhang, T., Liu, Z., Long, X., Wei, Z. et. al. (2014). High-Performance Hole-Extraction Layer of Sol-Gel-Processed NiO Nanocrystals for Inverted Planar Perovskite Solar Cells. *Angewandte Chemie International Edition*, 53 (46), 12571–12575. doi: <https://doi.org/10.1002/anie.201405176>
- Kim, G.-W., Shinde, D. V., Park, T. (2015). Thickness of the hole transport layer in perovskite solar cells: performance versus reproducibility. *RSC Advances*, 5 (120), 99356–99360. doi: <https://doi.org/10.1039/c5ra18648j>
- Marinova, N., Tress, W., Humphry-Baker, R., Dar, M. I., Bojinov, V., Zakeeruddin, S. M. et. al. (2015). Light Harvesting and Charge Recombination in CH₃NH₃PbI₃ Perovskite Solar Cells Studied by Hole Transport Layer Thickness Variation. *ACS Nano*, 9 (4), 4200–4209. doi: <https://doi.org/10.1021/acs.nano.5b00447>

16. Manders, J. R., Tsang, S.-W., Hartel, M. J., Lai, T.-H., Chen, S., Amb, C. M. et. al. (2013). Solution-Processed Nickel Oxide Hole Transport Layers in High Efficiency Polymer Photovoltaic Cells. *Advanced Functional Materials*, 23 (23), 2993–3001. doi: <https://doi.org/10.1002/adfm.201202269>
17. Dai, B., Fu, L., Liao, L., Liu, N., Yan, K., Chen, Y., Liu, Z. (2011). High-quality single-layer graphene via reparative reduction of graphene oxide. *Nano Research*, 4 (5), 434–439. doi: <https://doi.org/10.1007/s12274-011-0099-8>
18. Wang, Y., Hu, Y., Han, D., Yuan, Q., Cao, T., Chen, N. et. al. (2019). Ammonia-treated graphene oxide and PEDOT:PSS as hole transport layer for high-performance perovskite solar cells with enhanced stability. *Organic Electronics*, 70, 63–70. doi: <https://doi.org/10.1016/j.orgel.2019.03.048>
19. Schniepp, H. C., Li, J.-L., McAllister, M. J., Sai, H., Herrera-Alonso, M., Adamson, D. H. et. al. (2006). Functionalized Single Graphene Sheets Derived from Splitting Graphite Oxide. *The Journal of Physical Chemistry B*, 110 (17), 8535–8539. doi: <https://doi.org/10.1021/jp060936f>
20. McAllister, M. J., Li, J.-L., Adamson, D. H., Schniepp, H. C., Abdala, A. A., Liu, J. et. al. (2007). Single Sheet Functionalized Graphene by Oxidation and Thermal Expansion of Graphite. *Chemistry of Materials*, 19 (18), 4396–4404. doi: <https://doi.org/10.1021/cm0630800>
21. Liu, D., Kelly, T. L. (2013). Perovskite solar cells with a planar heterojunction structure prepared using room-temperature solution processing techniques. *Nature Photonics*, 8 (2), 133–138. doi: <https://doi.org/10.1038/nphoton.2013.342>
22. Kim, H.-S., Lee, C.-R., Im, J.-H., Lee, K.-B., Moehl, T., Marchioro, A. et. al. (2012). Lead Iodide Perovskite Sensitized All-Solid-State Submicron Thin Film Mesoscopic Solar Cell with Efficiency Exceeding 9%. *Scientific Reports*, 2 (1). doi: <https://doi.org/10.1038/srep00591>
23. Tseng, Z.-L., Chiang, C.-H., Chang, S.-H., Wu, C.-G. (2016). Surface engineering of ZnO electron transporting layer via Al doping for high efficiency planar perovskite solar cells. *Nano Energy*, 28, 311–318. doi: <https://doi.org/10.1016/j.nanoen.2016.08.035>
24. Das, R., Hamid, S., Ali, M., Ramakrishna, S., Yongzhi, W. (2014). Carbon Nanotubes Characterization by X-ray Powder Diffraction – A Review. *Current Nanoscience*, 11 (1), 23–35. doi: <https://doi.org/10.2174/1573413710666140818210043>
25. Dobiášová, L., Starý, V., Glogar, P., Valvoda, V. (1999). Analysis of carbon fibers and carbon composites by asymmetric X-ray diffraction technique. *Carbon*, 37 (3), 421–425. doi: [https://doi.org/10.1016/s0008-6223\(98\)00207-3](https://doi.org/10.1016/s0008-6223(98)00207-3)